RSC Advances

PAPER

View Article Online
View Journal | View Issue

Cite this: *RSC Adv.*, 2025, **15**, 2850

Design, synthesis, anti-inflammatory evaluation, and molecular docking studies of novel quinazoline-4(3*H*)-one-2-carbothioamide derivatives†

Le Thanh Hang Nguyen,[a] Dinh Hoang Vu,[a] Minh Quan Pham,[bc] Quoc Anh Ngo*[d] and Ngoc Binh Vo*[d]

In this paper, a series of novel quinazoline-4(3*H*)-one-2-carbothioamide derivatives (**8a–p**) were designed and synthesized *via* the Wilgerodt–Kindler reaction between 2-methylquinazoline-4-one **10** and amines using S_8/DMSO as the oxidizing system. Their characteristics were confirmed by IR, NMR, HRMS spectra, and their melting point. These novel derivatives (**8a–p**) were evaluated for their anti-inflammatory activity by inhibiting NO production in lipopolysaccharide (LPS)-activated RAW 264.7 macrophage cells. Compounds **8d** (IC_{50} = 2.99 μM), **8g** (IC_{50} = 3.27 μM), and **8k** (IC_{50} = 1.12 μM) exhibited potent inhibition of NO production compared to the standard drug dexamethasone (IC_{50} = 14.20 μM). Compound **8a** (IC_{50} = 13.44 μM) exhibited NO inhibition comparable to dexamethasone. Structure–activity relationship (SAR) studies indicated that the presence of both the thioamide functional group (NH–C=S) directly attached to the phenyl ring containing halogen substituents (4-Cl, **8d**), (4-Br, **8g**) and (4-CF_3, **8k**), is responsible for the potent anti-inflammatory activity of these novel quinazolinone derivatives. Computational modeling studies revealed that compounds **8d**, **8g**, and **8k** are potent inhibitors of TLR4 signaling through the formation of hydrophobic interactions and are stabilized by hydrogen bonds. Replacing the thioamide (**8k**) with an amide (**8q**) resulted in an 83-fold decrease in NO inhibitory potency. This highlights the important role of H-bonding involving the thioamide group. The structural shape difference results in favorable interactions of quinazolinones containing thioamide linkers compared to amide linkers to the target receptor. Furthermore, the ADMET profiles and physicochemical properties of these three lead compounds were predicted to meet the criteria for drug-like properties. Therefore, these compounds may be potential candidates for the treatment of many inflammatory diseases associated with immune disorders.

Received 30th December 2024
Accepted 21st January 2025

DOI: 10.1039/d4ra09094b

rsc.li/rsc-advances

Introduction

Inflammation is a complex pathophysiological process caused by the overproduction of inflammatory mediators such as nitric oxide (NO), prostaglandin E_2 (PGE_2), as well as inflammatory cytokines, such as tumor necrosis factor-α (TNF-α), interleukin-6 (IL-6), and interleukin-1β (IL-1β).[1] Overproduction of these inflammatory mediators is closely linked to several diseases such as atherosclerosis, diabetes, cancer, neuropsychiatric disorders, and various inflammatory disorders such as rheumatoid arthritis, inflammatory bowel disease, rheumatoid arthritis, and psoriasis.[2–4] Among them, NO has emerged as a key mediator of inflammation, playing an important role in both acute and chronic inflammatory diseases.[5,6] NO is produced by three isoforms of nitric oxide synthase (NOS) (iNOS, eNOS, and nNOS), under stimulation by proinflammatory cytokines, or bacterial lipopolysaccharide (LPS) in many cell types including macrophages.[5,6] LPS is a major component of the membrane of Gram-negative bacteria, plays a role in stimulating the production of inflammatory mediators and is recognized by toll-like receptor 4 (TLR4).[7] Overproduction of NO has been implicated in the progression of several inflammatory disorders in the joints, intestines, and lungs.[8] Most of the current anti-inflammatory drugs, along with their therapeutic properties, are associated with some side effects at different levels such as toxicity to the liver, and gastrointestinal

[a]*School of Chemistry and Life Sciences, Hanoi University of Science and Technology, 1 Dai Co Viet Street, Hanoi, Vietnam*
[b]*Institute of Natural Products Chemistry (INPC), Vietnam Academy of Science and Technology (VAST), Hanoi, Vietnam*
[c]*Graduate University of Science and Technology (GUST), Vietnam Academy of Science and Technology (VAST), Hanoi, Vietnam*
[d]*Institute of Chemistry, Vietnam Academy of Science and Technology, Hanoi, Vietnam. E-mail: binhvn.tq@gmail.com*

† Electronic supplementary information (ESI) available. See DOI: https://doi.org/10.1039/d4ra09094b

tract, risks for cardiovascular disease, kidney disease, and hypertension.[9,10] Therefore, researchers today aim to design new-generation anti-inflammatory drugs with strong anti-inflammatory properties and low toxicity.[10]

Quinazolinones have emerged as an important pharmacological scaffolds in organic chemistry, possessing a wide range of biological properties such as anti-inflammatory and analgesic, anticonvulsant, antibacterial, antifungal, antituberculosis, anticancer, anti-HIV, anti-leishmanicidal activity.[11] Among them, the quinazolin-4(3*H*)-one scaffold (Fig. 1) is the most common and important of the quinazolinones[12] that we selected for this study due to its remarkable anti-inflammatory activity.[11,13] Proquazone (**1**) and fluproquazone (**2**) are well-known NSAIDs containing a quinazolinone scaffold. In addition, rutaecarpine (**3**) is a natural quinazolinone derivative from *Evodia rutaecarpa* with anti-inflammatory activity, highly selective for COX-2 inhibition,[14] in contrast to synthetic COX-2 inhibitors such as etoricoxib and celecoxib, rutecarpine has beneficial effects on some cardiovascular diseases.[15] In addition, several reports have shown that substitutions at position 2 or 3 of the quinazoline nucleus significantly affect anti-inflammatory activity.[13,16–21] On the other hand, the molecular structure of quinazolin-4(3*H*)-one scaffold shows that they are lipophilic,[13,22] which will facilitate the design of anti-inflammatory drugs.[23] Sutthichat Kerdphon *et al.* synthesized and studied the molecular docking of quinazolinones with an aliphatic substitution at the C-2 position, which showed good to excellent inhibition of inflammatory gene expression, including COX-2, iNOS, and IL-1β mRNA through inhibition of nuclear factor κB (NF-κB). Molecular docking studies showed that the quinazolin-4(3*H*)-ones binding to the receptor was facilitated by hydrogen bonding, hydrophobic, and electrostatic interactions as well as π–π and amide–π interactions.[21]

Recent studies have shown that the introduction of linkers such as ester (compound **4**, Fig. 1) or amide (compound **5**, Fig. 1) between the aromatic/heterocyclic ring and the central heterocycle leads to improved hydrogen bond formation with the enzyme active site, resulting in compounds with potent anti-inflammatory activity and high selectivity for COX-2 inhibition.[19,24–26] Kambappa Vinaya *et al.*[27] synthesized a (4-hydroxyphenyl)(2,4-dimethoxyphenyl) methanone derivative **6** with a thioamide linker to a 4-fluorophenyl aromatic ring that exhibited potent anti-inflammatory activity at 30 mg kg^{-1} p.o. than the standard drug diclofenac sodium. Structural studies indicated that both the functional linkage (–CS–NH–) and the electron-withdrawing groups attached to the phenyl ring were responsible for the potent anti-inflammatory activity of the synthesized derivatives.

The thioamide functional group is a bioisostere of the amide functional group, which is believed to enhance the chemical stability and biological activity of amide-functionalized drug molecules.[28] Thioamides are thought to be better hydrogen bond donors than amides.[29] Isosteric substitution of an amide donor with a thioamide can increase ligand affinity due to

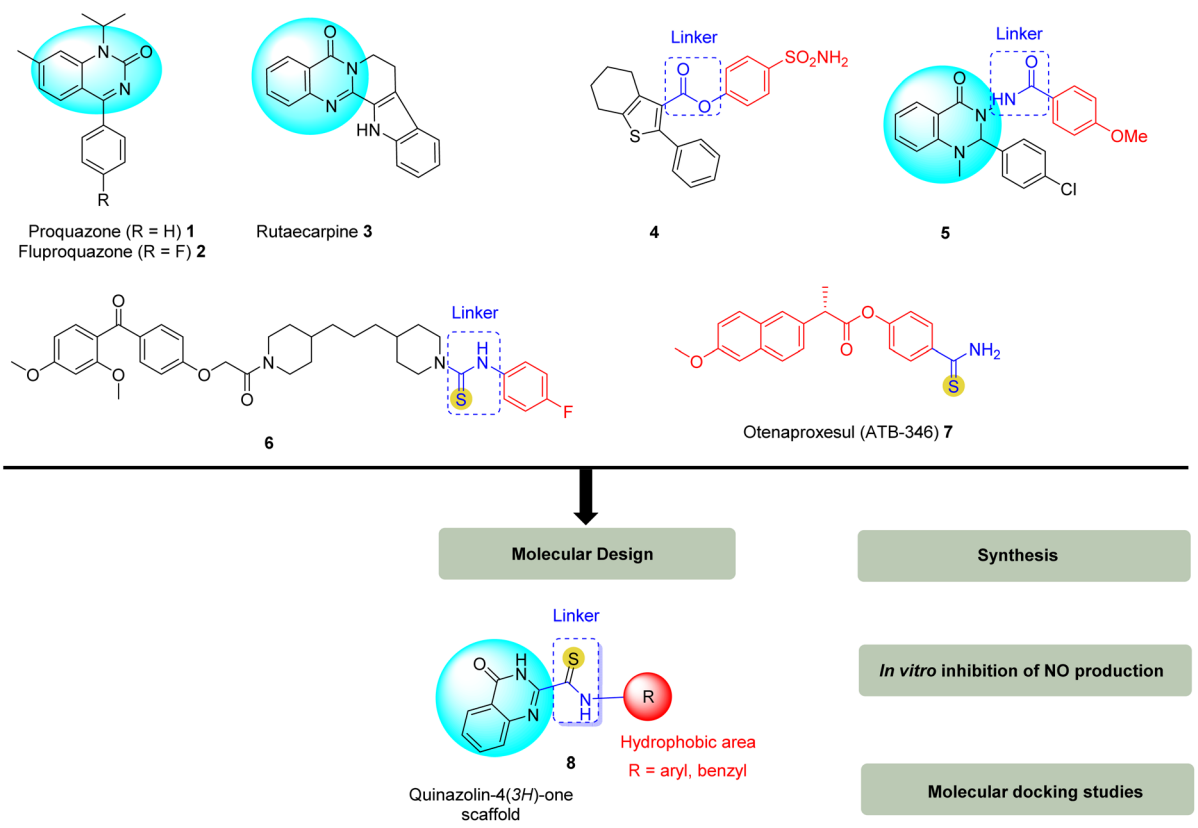

Fig. 1 Structure of the proquazone **1**, fluproquazone **2**, rutaecarpine **3**, some potent anti-inflammatory agents based on the ester linker **4**, amide **5**, thioamide **6**, **7**, and the designed molecule **8**.

enhanced n → π* electron transfer, as well as impart conformational stability to the thioamide.[30] Furthermore, the substitution of amide with thioamide is beneficial for permeation, as well as stability under physiological conditions.[31,32] In addition, compounds containing the thioamide function have attracted great attention in medicinal chemistry due to their broad spectrum of biological activity,[33–35] useful synthetic substrates in the synthesis of heterocyclic rings,[36] suitable stability, and low toxicity.[34] A recent review of thioamides as small molecule therapeutic agents in medicinal chemistry showed that thioamides exhibit pharmacological activities and pharmacokinetic properties superior to their isosteres.[35] In the field of anti-inflammatory drug design, combining NSAID pharmacological scaffolds with thioamide groups that act as H_2S-releasing agents is an effective strategy to develop anti-inflammatory drugs with dual effects, *i.e.*, increasing the efficacy of the parent compound while reducing its side effects.[37–39] Among them, otenaproxesul (ATB-346) (compound 7, Fig. 1) is a new orally administered NSAID that releases hydrogen sulfide (H_2S) into the gastrointestinal tract and is being developed by Antibe Therapeutics.[40,41] Therefore, many new synthetic methods have been developed to access thioamide compounds.[42,43] Recently, we reported a useful method for the synthesis of thioamides through the use of the S_8/DMSO system that promotes the direct oxidative coupling of active methylhetarene with amines under mild conditions, with low sulfur content.[44]

Based on these findings, we selected quinazolin-4(3*H*)-one as the pharmacological scaffold for anti-inflammatory activity, the thioamide functional group attached with hydrophobic moieties such as aryl/benzyl was introduced at the C-2 position of the quinazolinone scaffold to enhance the binding affinity to the biological target. Different substituents on the phenyl ring were also introduced to study the structure–activity relationship (SAR). The novel quinazoline-4(3*H*)-one-2-carbothioamide derivatives were evaluated for anti-inflammatory activity through NO inhibition. Furthermore, *in silico* studies on physicochemical properties and ADMET of the compounds were also carried out to evaluate their potential in drug development.

Results and discussion

Chemistry

Our recent work has revealed a useful method to approach thioamide derivatives by promoting the direct oxidative coupling reaction of active methylhetarene with amine using S_8/DMSO under mild temperatures.[44] Following these results, we selected the molecule 2-methylquinazolin-4(3*H*)-one **10** as the methylhetarene moiety to apply this reaction. Firstly, compound **10** was synthesized based on a simple method previously reported by Sun *et al.*,[45] in which 2-aminobenzamide **9** was refluxed in excess ethanol for 48 h in the presence of TBHP as an oxidant after removal of the solvent under reduced pressure and the crude product was crystallized in ethyl acetate to afford compound **10** in 65% yield (Scheme 1).

In the IR spectrum of compound **10**, signals of important functional groups on the quinazolin-4(3*H*)-one nucleus were observed at 3446 cm^{-1} (N–H, amide) and 1672 cm^{-1} (C=O, amide). In the ^{1}H NMR spectrum of **10**, two singlet signals at 12.17 ppm and 2.35 ppm were attributed to the N–H proton of the amide group and the proton of the methyl group (–CH_3). In summary, the IR and NMR data of compound **10** were consistent with the published data of this compound.[46,47] In the second step (Scheme 1), new quinazoline-4(3*H*)-one derivatives (**8a–p**) were synthesized *via* the Wilgerodt–Kindler reaction of compound **10** with arylamines **11a–n**, using S_8/DMSO as the oxidizing agent, at 110 °C for 16 h (ii) or with benzylamines **11o**, **11p** in the presence of S_8/DMSO and CH_3COOH, at 100 °C, 16 h (iii). Fifteen new quinazoline-4(3*H*)-one-2-carbothioamide derivatives (**8a–p**) containing the thioamide group were synthesized in yields ranging from 28% to 82%. Among them, the reaction of **10** with arylamine reagents **11a–n** (from 42%–82%) gave higher yields than with benzylamines **11o**, **11p** (from 28–36%). Amide compound **8q** was also synthesized *via* the reaction of **10** and arylamine **11k** using S_8/DMSO system as an oxidizing agent and catalyzed by $FeCl_2 \cdot 4H_2O$ (5 mol%), at 120 °C for 16 h.[48] Amide **8q** was obtained in a moderate yield of 43%. The structures of all the synthesized compounds were characterized by melting point, IR, NMR, and LC-MS spectra.

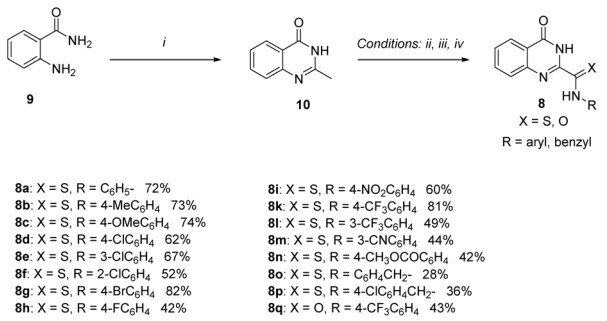

Scheme 1 Synthesis of novel quinazoline-4(3*H*)-one-2-carbothioamide derivatives (**8a–p**) and quinazoline-4(3*H*)-one-2-carboxamide **8q**. Reagents and conditions: (i) EtOH, *tert*-butyl hydroperoxide (TBHP), reflux, 48 h; (ii) for **8a–n**: arylamine (**11a–n**), S_8, DMSO, 110 °C, 16 h; (iii) for **8o**, **8p**: benzylamines (**11o**, **11p**), S_8, DMSO, CH_3COOH, 100 °C, 16 h; (iv) for **8q**: 4-(trifluoromethyl)aniline (**11k**), S_8, DMSO, $FeCl_2 \cdot 4H_2O$ (5 mol%), 120 °C, 16 h.

In the IR spectrum of the new quinazolin-4(3*H*)-ones **8a–p**, in addition to the characteristic stretching bands for the amide functional group on the quinazolin-4(3*H*)-one nucleus such as N–H at 3481–3359 cm^{-1} and C=O at 1709–1603 cm^{-1}, additional stretching bands for the thioamide functional group appeared, namely N–H at 3278–3190 cm^{-1} and C=S at 1110–1023 cm^{-1}. In the ^{1}H NMR spectrum of quinazolin-4(3*H*)-ones **8a–p**, the singlet signal at 12.70–10.83 ppm was assigned to the N–H proton (amide group) on the quinazolinone nucleus, the new singlet signal appeared at 12.06–10.08 ppm demonstrating the presence of the N–H proton (thioamide functional group). The ^{1}H NMR spectra of compounds **8o** and **8p** with benzylamine reagent clearly showed proton signals –CH_2– at 5.00 ppm (d, J = 5.8 Hz, 2H) for **8o** and 4.98 ppm (d, J = 5.9 Hz, 2H) for **8p**. In the ^{13}C NMR spectra of quinazolin-4(3*H*)-ones **8a–p**, characteristic peaks of carbon C=S (thioamide group) at 186–178 ppm and carbon C=O (amide group) at 161.16–160.4 ppm were observed. Additionally, the presence of carbon signal of

a methylene group (–CH_2–) in compounds **8o** and **8p** could be observed at 50.38 ppm and 52.29 ppm, respectively. For compound **8q**, the IR spectrum showed peaks at 3332 and 3188 cm^{-1} assigned to the N–H protons of the amide groups and 1669 cm^{-1} characteristic of the stretching vibration peak of the amide C=O bond. In the ^{13}C NMR spectrum of **8q**, the carbon chemical shift (C=O, amide) was found in the upfield region (at 161.43 and 159.14 ppm) relative to the resonance of carbon (C=S, thioamide) at 180.46 ppm in **8k**.[29] Finally, the stereochemical configuration of the synthesized compounds **8a–p** was examined through the NOESY spectrum in the $CDCl_3$ solvent of compound **8k**. In the NOESY spectrum of compound **8k**, only one cross peak of the interaction of the N–H (amide) proton with H-2′ and H-6′ could be observed. Furthermore, the morphology and crystal structure of the analogous compound[49] indicated that the stereochemical configuration of compounds **8a–p** was the (*Z*) configuration. TOF MS ESI^+ spectrum shows characteristic $[M + H]^+$ peak corresponding to the molecular weight of the synthesized compound (see in ESI†).

Anti-inflammatory activity

All synthesized quinazolinone compounds **8a–q** were tested for their anti-inflammatory activity by inhibiting nitric oxide (NO) production on mouse macrophages RAW 264.7, activated by lipopolysaccharide (LPS). Dexamethasone was used as the reference standard drug for our screening studies. The results of the *in vitro* NO production inhibition assay are presented in Table 1.

The IC_{50} value data of the compounds in Table 1 showed that the compounds **8d**, **8g**, and **8k** exhibited potent anti-inflammatory activity compared to the positive control drug dexamethasone (IC_{50} = 14.20 μM) with IC_{50} values of 2.99, 3.27, and 1.12 μM, respectively. Compound **8a** (IC_{50} = 13.44 μM) exhibited anti-inflammatory activity comparable to dexamethasone. Compounds **8b**, **8c**, **8e**, **8i**, and **8q** showed weak inhibitory activity on the production of inflammatory mediator NO with IC_{50} in the range of 72.89–96.09 μM. The remaining compounds including **8f**, **8h**, **8l**, **8m**, **8n**, **8o**, and **8p** did not show anti-inflammatory activity.

Table 1 Inhibitory ability of NO production of synthesized derivatives **8a–q**

Entry	Compounds	X	R	IC_{50} (μM) ± SD[a]
1	**8a**	S	Ph	13.44 ± 0.70
2	**8b**	S	4-MeC_6H_4	72.89 ± 3.50
3	**8c**	S	4-$OMeC_6H_4$	87.35 ± 3.07
4	**8d**	S	4-ClC_6H_4	2.99 ± 0.19
5	**8e**	S	3-ClC_6H_4	96.09 ± 4.93
6	**8f**	S	2-ClC_6H_4	>160.96
7	**8g**	S	4-BrC_6H_4	3.27 ± 0.13
8	**8h**	S	4-FC_6H_4	>100
9	**8i**	S	4-$NO_2C_6H_4$	88.82 ± 2.56
10	**8k**	S	4-$CF_3C_6H_4$	1.12 ± 0.11
11	**8l**	S	3-$CF_3C_6H_4$	>100
12	**8m**	S	3-CNC_6H_4	>100
13	**8n**	S	4-$CH_3OCOC_6H_4$	>100
14	**8o**	S	$C_6H_4CH_2^-$	>100
15	**8p**	S	4-$ClC_6H_4CH_2^-$	>100
16	**8q**	O	4-$CF_3C_6H_4$	93.32 ± 5.46
17	Dexamethasone			14.20 ± 0.54

[a] Data are expressed as mean IC_{50} ± SD (μM), n = 3, using TableCurve 2Dv4 software for data calculation.

Structure–activity relationship (SAR)

To study SAR, we introduced various substituents including both electron-withdrawing and electron-donating groups attached to the phenyl ring as substitutes linked to the thioamide group (Fig. 2). First, the simultaneous presence of both the thioamide linker and the unsubstituted phenyl ring in **8a** showed good inhibition of NO production, comparable to the reference drug. The introduction of electron-withdrawing groups containing halogen elements such as –Cl (**8d**), –Br (**8g**), and –CF_3 (**8k**) at the *para*-position on the phenyl ring further enhanced the *in vitro* anti-inflammatory activity of these derivatives, except for the case of the 4-F substituent (**8h**) which did not show activity. However, moving the –Cl substituent from the *para*- (**8d**) to the *meta*- (**8e**), *ortho*- (**8f**), or –CF_3 to the *meta*- (**8l**) position results in decreased or loss of activity. In general, the introduction of other electron-withdrawing substituents into the phenyl ring such as (4-NO_2, **8i**), (3-CN, **8m**), and (4-CH_3OCO, **8n**) all showed low or no NO inhibitory activity.

The introduction of electron-donating groups such as –CH_3 (**8b**) and –OCH_3 (**8c**) into the phenyl ring reduced the NO inhibitory activity. Finally, the two designed compounds **8o** and **8p** containing the benzyl group did not show anti-inflammatory activity. This suggests that the conjugation of the thioamide linker directly attached to the aromatic ring influences the anti-inflammatory activity. In summary, the presence of both the thioamide group (NH–C=S) and electron-withdrawing halogen substituents (–CF_3, –Cl, –Br) at the *para*-position on the phenyl ring is thought to increase the lipophilicity of the molecule,[10,26,50,51] which would enhance cell permeability and thereby enhance the NO production inhibitory activity of these compounds. In addition, we also attempted to explore the isosteric substitution strategy based on the **8k** compound with the best NO inhibitory activity. The results showed that the amide isostere **8q** had a strongly reduced potency.

Molecular docking studies

Statistical results suggest that predicting various molecular properties early in the discovery and development process is

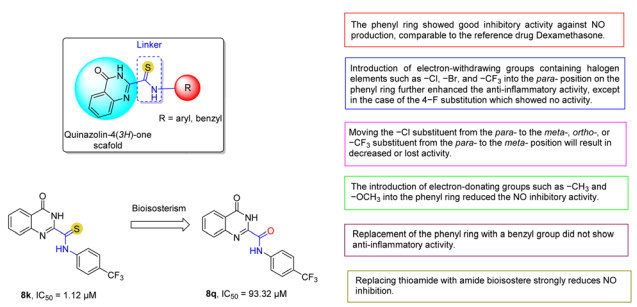

Fig. 2 Summary of SAR studies of novel quinazoline-4(3*H*)-one-2-carbothioamide derivatives.

a crucial step.[52] Thus, all ligands were assessed for Lipinski's Rule of Five parameters and drug-likeness properties using admetSAR1 and ProTox-III cheminformatic online web servers.[53] Obtained results are presented in Table 2.

The results of Lipinski's Rule of Five assessment show that all studied compounds are favorable for oral drug development, each having fewer than two condition violations. Additionally, pharmacokinetic parameters and toxicity prediction results, combined with docking studies, provide valuable information for evaluating potential compounds with inhibitory abilities and drug-like properties for further development. The calculated properties showed interesting results on the toxicity scale. From Table 2, five compounds including **8a**, **8c**, **8d**, **8g**, **8i**, and **8q** were classified as low-toxic (rank 3). The other ten candidates were positioned at rank 4 and considered safe, including compounds **8b**, **8e**, **8f**, **8h**, **8k**, **8l**, **8m**, **8n**, **8o**, and **8p**. Moreover, it was reported that compounds with good oral bioavailability typically have a total polar surface area (TPSA) ranging from 70 to 140 Å^2, human intestinal absorption (HIA) values above 50%, and contain 12 or fewer hydrogen bond donors (HBD) and acceptors (HBA).[54] In this study, all compounds were observed to have TPSA values within the range 70–140 Å^2, and the HIA percentage ranged from 78.24 to 96.72%. From physicochemical properties, these compounds are likely to be membrane permeable and easily absorbed in the human body based on satisfaction of the criteria of drug-like properties thus, demonstrating suitability in oral drug development.

AutoDock4 is among the most popular docking software, with over 6000 citations since 2010.[55–57] It is a valuable tool for rapidly predicting the binding affinity of ligands to specific protein or enzyme targets. In this scenario, AutoDock4 has been utilized in searching for potential mechanisms of the bioactive compounds. The docking scores are shown in Table 2. Using Cheng–Prusoff's formula, the K_i inhibition constant is calculated as follows:

$$K_i = \frac{IC_{50}}{1 + \frac{[S]}{K_m}} = \exp\left(\frac{\Delta G}{RT}\right) \rightarrow IC_{50} = \exp\left(\frac{\Delta G}{RT}\right) + \exp\left(\frac{\Delta G}{RT}\right) \times \frac{[S]}{K_m} \quad (1)$$

Assuming the IC_{50} value equals K_i, the experimental binding free energy could be derived from the aforementioned formula as follows: $\Delta G_{exp} = RT\ln(K_i) = RT\ln(IC_{50})$ where $R = 1.987 \times 10^{-3}$ (kcal K^{-1} mol^{-1}); $T = 300$ (K) and inhibition constant K_i is measured in moles. Energy is measured in kilocalories per mole. Taking into account compounds that are assumed to be bioactive (IC_{50} less than 100 μM), the plotting of experimental binding free energies against the computed values gave a relatively high correlation coefficient of $R^2 = 0.79$ (Fig. 3).

According to the ranking criteria of Autodock4, the more negative docking energy suggests the higher binding affinity of the compound towards the targeted receptor.[58] The docking score of dexamethasone was −7.10 kcal mol^{-1}, thus, any ligand

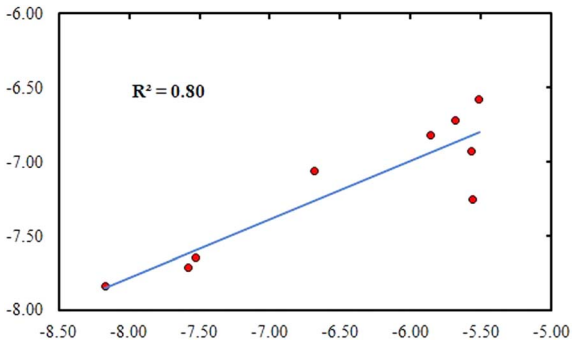

Fig. 3 The correlation between experimental and computational binding free energies.

Table 2 The docking score and Lipinski parameters of studied compounds **8a–q**

CP IDs	Dock score (kcal mol^{-1})	HBA (≤10)	HBD (≤5)	Log *P* (−4.0–5)	TPSA[a] (0–150) Å	HIA[b] (%)	LD_{50} (mg kg^{-1})	Toxic class[c]
8a	−7.06	4	2	2.899	83.66	88.67	200	3
8b	−6.72	4	2	3.208	88.40	93.25	400	4
8c	−6.93	5	2	2.908	90.21	88.67	200	3
8d	−7.71	4	2	3.552	88.67	89.98	250	3
8e	−6.58	4	2	3.552	88.67	89.98	580	4
8f	−6.02	4	2	3.552	88.67	89.27	470	4
8g	−7.65	4	2	3.661	91.36	86.26	200	3
8h	−6.51	4	2	3.038	83.62	90.03	390	4
8i	−7.25	6	2	2.807	90.32	87.25	200	3
8k	−7.84	4	2	3.918	88.66	96.72	425	4
8l	−6.09	4	2	3.918	88.66	96.72	2000	4
8m	−6.15	5	2	2.771	88.38	87.39	400	4
8n	−5.87	6	2	2.686	95.00	78.24	1600	4
8o	−6.38	4	2	2.577	86.88	92.49	900	4
8p	−6.14	4	2	3.230	91.89	93.41	500	4
8q	−7.32	5	2	3.117	81.07	92.69	200	3
Dexamethasone	−7.10	5	3	1.895	99.94	99.20	3000	5

[a] TPSA: molecular total polar surface area. [b] HIA: human intestinal absorption. [c] Toxicity prediction class: 1 → 6 (high toxicity to non-toxic).

whose docking energy is close to this value or more negative would be considered a potential inhibitor. Obtained results indicate that 3 out of 15 studied compounds could be assumed as "HITs" based on their dock score, including **8d**, **8g**, and **8k**. The stereoview of the binding mode of three HIT ligands is depicted in Fig. 4.

Previously, several studies have reported potential inhibitors of TLR4 signaling using computational tools. Thus, in this research, the molecular docking simulation was utilized to identify possible binding sites on TLR4 for potential compounds.[59–61] It is observed that dexamethasone and three HIT compounds did not bind to the hydrophobic pocket in MD-2, where LPS bridges TLR4 and MD-2 to initiate signal transduction. It was bound to a cleft mainly constructed by TLR4. Fig. 3A showed that residues Arg337, Gln339, Met358, Lys360 and Arg380 from TLR4, along with His96 from MD-2, formed a smooth surface. The twisted structures of **8d**, **8g**, and **8k** fit this shape perfectly and were closely attached to the surface.

The binding conformation of dexamethasone revealed that Met358, Asn359, and Lys360 formed three H-bonds with this ligand, the interaction was further stabilized through hydrophobic binding with Arg380. Of all the docked results, compound **8k** exhibited the highest binding affinity (-7.84 kcal mol^{-1}). Binding orientation analysis of **8k** shows that Met358, Arg380, Asn381, and Phe406 were the key residues that participated in hydrophobic interaction. The interaction was further stabilized through H-bonds with Arg337 and Lys360. In the docked pose of **8d**, the hydrophobic pockets

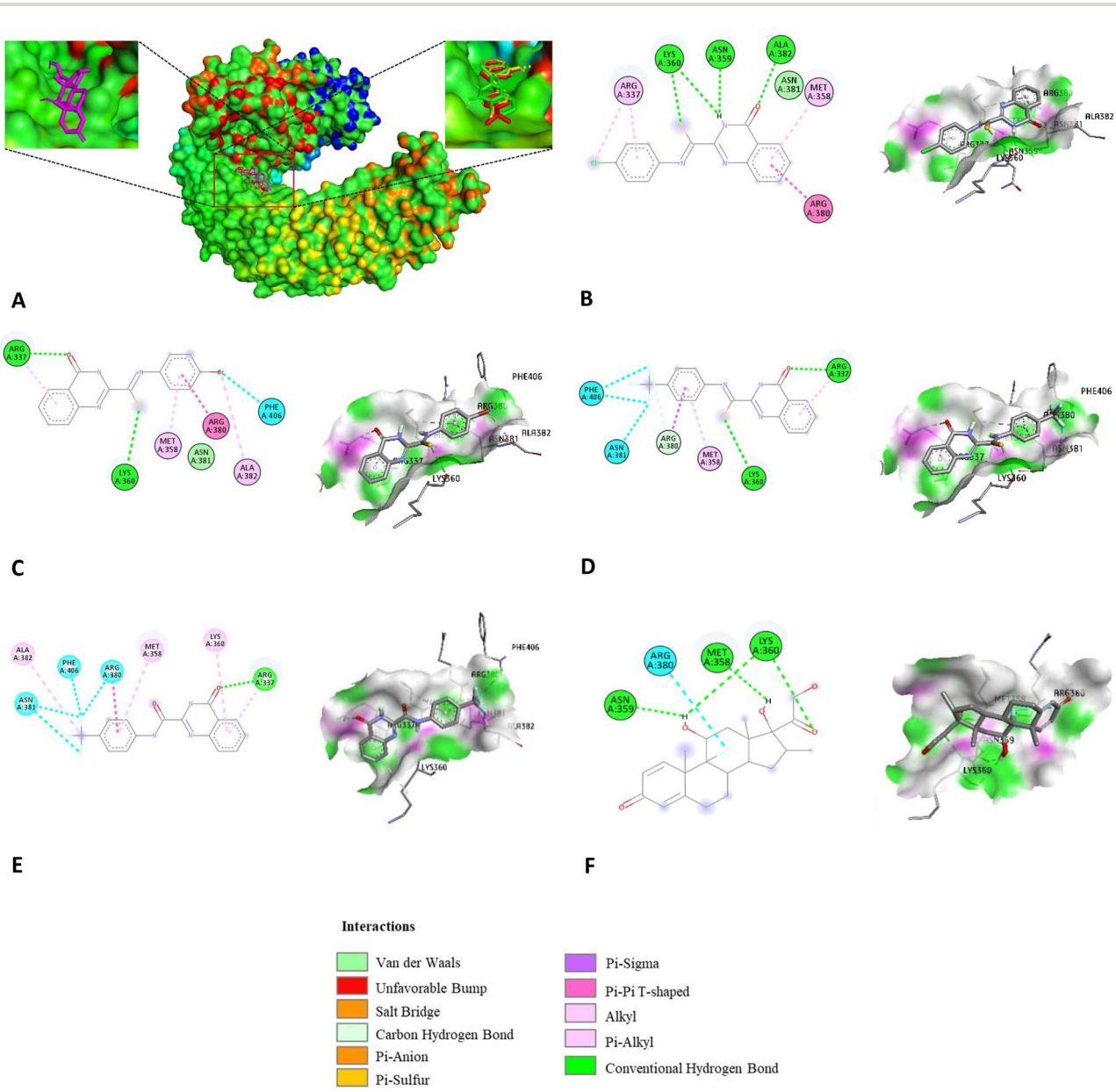

Fig. 4 Binding conformation of studied compounds revealed by molecular docking simulations. (A) HIT compounds bind to a smooth region in TLR4, adjacent to its contact interface with MD-2: dexamethasone-magenta color, **8d**-green color, **8g**-yellow color, **8k**-red color; (B) dock pose of **8d**; (C) dock pose of **8g**; (D) dock pose of **8k**; (E) dock pose of **8q**; (F) dock pose of dexamethasone.

formed with this ligand involving residues Arg337, Met358, Arg380, and Asn381. The interaction is further strengthened through three conventional hydrogen bonds with Asn359, Lys360, and Ala382. An array of hydrophobic interactions was observed as contributed by Met358, Arg380, Asn381, and Ala382 to the binding with compound **8g**. Also, the hydrogen bonds were constituted from interaction with Arg337 and Lys360. The amide compound **8q** showed a lower binding affinity (-7.32 kcal mol^{-1}) than the corresponding thioamide isostere **8k**, respectively. Binding analysis of **8q** showed that it also participated in hydrophobic interactions with amino acids such as Ala382, Phe406, Arg380, Asn381, Met358, and Lys360. The carbonyl group in the quinazoline ring formed hydrogen bonds with Arg337 residues. However, the amide bond inserted into the quinazoline ring at the C-2 position did not participate in interactions with any amino acids. In contrast to the twisted conformation of **8k**, amide **8q** appears to have a planar conformation (Fig. 4), in which case this conformation appears not to be optimal for binding to the active site. This may explain the lower binding affinity and NO inhibitory potency compared to the **8k** thioamide bioisostere.

Molecular docking simulations further revealed that HIT compounds could inhibit TLR4 signaling through direct interaction, with the twisted structure being crucial in this process. Unlike the interaction between LPS and TLR4, the three most potent compounds did not occupy the binding site in MD-2; instead, they bound to an adjacent smooth region in TLR4. This likely undermined the formation of the primary contact interface between TLR4 and MD-2 and the recognition of LPS. Given the significant role of TLR4 in inflammation and immunity, these findings suggest that they could have potent applications in treating many inflammatory diseases related to immune disorders.

Experimental

Chemistry

All chemicals and solvents used as analytical reagents were supplied by commercial chemical companies and were used directly without further purification steps. The melting temperatures of the compounds were recorded by a Krüss M5000 melting point meter at default settings. A PerkinElmer Spectrum Two FT-IR spectrometer was used to record the IR spectra, using the pellet method with KBr. ^{1}H NMR (600 MHz) and ^{13}C NMR (125/150 MHz) spectra were recorded using Bruker AV-600 and Bruker AV-500 spectrometers with TMS as standard, $CDCl_3$ and DMSO-d_6 as solvents. NMR data are described in terms of chemical shifts (ppm), multiplets: s (singlet), d (doublet), t (triplet), q (quartet), m (multiplet), coupling constants (Hz), and integration. High-resolution mass spectral data of all compounds were collected in ESI positive mode using a SCIEX X500R QTOF high-resolution mass spectrometer. Reactions were monitored by thin-layer chromatography (TLC) using aluminum TLC plates pre-coated with silica gel 60 F_{254}, 0.25 mm (Merck) and detected by UV light at 254 nm. The purity of HIT compounds **8d**, **8g**, and **8k** was >94% as determined by high-performance liquid chromatography (HPLC), (LC, Agilent 1100 series; column, Agilent C18, 170 Å, 4.6 × 150 mm, 5 μm; column temperature, 25 °C; mobile phase, solvent A, methanol, solvent B, water, gradient elution, 20–99% solvent A; flow rate, 1 mL min^{-1}; UV signals were recorded at 254 nm).

Synthesis of 2-methylquinazolin-4(3*H*)-one (10)

Compound **10** was synthesized based on a previously reported study[45] with some minor modifications. A solution of 2-aminobenzamide **9** (500 mg, 3.67 mmol), 2 mL of TBHP (70% in H_2O) (14.68 mmol), and 37 mL of absolute ethanol were refluxed for 48 h. The reaction progress was monitored and checked by TLC (ethyl acetate : *n*-hexane = 1 : 1, v/v). At the end of the reaction, the reaction mixture was dried under reduced pressure to obtain the crude product. The crude product was crystallized in ethyl acetate to obtain 382 mg of **10** as a white solid. The reaction yield was 65%.

2-Methylquinazolin-4(3*H*)-one (10).[47] White solid. Yield: 75%. M.p.: 233–234 °C (lit.[62] 235–239 °C). IR (KBr, cm^{-1}):[46] ν 3446 (N–H, amide), 3169, 3045, 2921, 1672 (C=O, amide), 1467, 1382, 1340, 1292, 1250, 1145, 887, 772. ^{1}H NMR (600 MHz, DMSO-d_6) δ 12.17 (s, 1H), 8.08 (dd, J = 7.9, 1.0 Hz, 1H), 7.76 (ddd, J = 8.3, 7.1, 1.6 Hz, 1H), 7.57 (d, J = 7.5 Hz, 1H), 7.45 (ddd, J = 8.1, 7.1, 1.2 Hz, 1H), 2.35 (s, 3H). ^{13}C NMR (150 MHz, DMSO-d_6) δ 162.18, 154.72, 149.44, 134.72, 127.04, 126.30, 126.13, 121.10, 21.90. HR-MS (ESI) calcd. For $C_9H_9N_2O$ [(M + H)$^+$]: 161.0715; found: 161.0708.

General procedure for the synthesis of 3,4-dihydroquinazoline-2-carbothioamide derivatives (8a–n)

A mixture of **10** (1.0 mmol), aryl amine **11a–n** (1.0 mmol), and sulfur (40 mg, 1.25 mmol) in DMSO (0.5 mL) was heated in a 7 mL test tube sealed with a rubber stopper, at 110 °C for 16 h. The crude mixture was purified by column chromatography on silica gel (acetone : *n*-hexane = 3% to 5%, v/v) to obtain **8a–n** compounds.[44]

4-Oxo-*N*-phenyl-3,4-dihydroquinazoline-2-carbothioamide (8a). Compound **8a** was synthesized by the above procedure using aniline **11a** as an arylamine. Yellow solid. Yield: 72%. M.p.: 141–142 °C. IR (KBr, cm^{-1}): ν 3434 (NH, amide), 3234 (N–H, thioamide), 3140, 3050, 1675 (C=O, amide), 1592, 1436, 1388, 1332, 1067 (C=S, thioamide), 825, 766. ^{1}H NMR (600 MHz, $CDCl_3$) δ 11.68 (s, 1H), 10.96 (s, 1H), 8.36 (d, J = 7.8 Hz, 1H), 8.06 (d, J = 7.4 Hz, 2H), 7.84 (d, J = 3.5 Hz, 2H), 7.63–7.57 (m, 1H), 7.51–7.47 (m, 2H), 7.35 (t, J = 7.4 Hz, 1H). ^{13}C NMR (150 MHz, $CDCl_3$) δ 179.44, 160.51, 146.56, 144.09, 137.83, 135.06, 129.23, 128.74, 128.24, 127.47, 127.16, 122.42, 122.25. HR-MS (ESI) calcd. For $C_{15}H_{12}N_3OS$ [(M + H)$^+$]: 282.0701; found: 282.0691.

4-Oxo-*N*-(*p*-tolyl)-3,4-dihydroquinazoline-2-carbothioamide (8b). Compound **8b** was synthesized by the above procedure using 4-methylaniline **11b** as an arylamine. Yellow solid. Yield: 73%. M.p.: 178–179 °C. IR (KBr, cm^{-1}): ν 3481 (N–H, amide), 3197 (N–H, thioamide), 3032, 2914, 1680 (C=O, amide), 1601, 1529, 1475, 1435, 1388, 1330, 1063 (C=S, thioamide), 819, 767. ^{1}H NMR (600 MHz, $CDCl_3$) δ 11.64 (s, 1H), 11.00 (s, 1H), 8.37 (d,

J = 7.8 Hz, 1H), 7.94 (d, J = 8.2 Hz, 2H), 7.84 (d, J = 4.1 Hz, 2H), 7.60 (dt, J = 8.1, 4.2 Hz, 1H), 7.30 (d, J = 8.1 Hz, 2H), 2.41 (s, 3H). ^{13}C NMR (150 MHz, $CDCl_3$) δ 178.99, 160.57, 146.64, 144.19, 137.62, 135.39, 135.03, 129.75, 128.67, 128.21, 127.17, 122.40, 122.22, 21.26. HR-MS (ESI) calcd. For $C_{16}H_{14}N_3OS$ [$(M + H)^+$]: 296.0858; found: 296.0845.

***N*-(4-Methoxyphenyl)-4-oxo-3,4-dihydroquinazoline-2-carbothioamide (8c).** Compound **8c** was synthesized by the above procedure using 4-methoxyaniline **11c** as an arylamine. Yellow solid. Yield: 74%. M.p.: 212–216 °C. IR (KBr, cm^{-1}): ν 3435 (N–H, amide), 3249 (N–H, thioamide), 2917, 2843, 1693 (C=O, amide), 1602, 1515, 1464, 1404, 1308, 1263, 1023 (C=S, thioamide), 826, 772. ^{1}H NMR (600 MHz, $CDCl_3$) δ 11.61 (s, 1H), 11.00 (s, 1H), 8.37 (d, J = 7.8 Hz, 1H), 8.00 (d, J = 9.1 Hz, 2H), 7.90–7.81 (m, 2H), 7.64–7.57 (m, 1H), 7.01 (d, J = 9.0 Hz, 2H), 3.87 (s, 3H). ^{13}C NMR (125 MHz, $CDCl_3$) δ 178.42, 160.58, 158.52, 146.66, 144.26, 135.05, 131.02, 128.64, 128.18, 127.17, 123.90, 122.38, 114.31, 55.59. HR-MS (ESI) calcd. For $C_{16}H_{14}N_3O_2S$ [$(M + H)^+$]: 312.0807; found: 312.0794.

***N*-(4-Chlorophenyl)-4-oxo-3,4-dihydroquinazoline-2-carbothioamide (8d).** Compound **8d** was synthesized by the above procedure using 4-chloroaniline **11d** as an arylamine. Pale yellow solid. Yield: 62%. M.p.: 203–205 °C. IR (KBr, cm^{-1}): ν 3364 (N–H, amide), 3266 (N–H, thioamide), 3089, 2920, 1685 (C=O, amide), 1602, 1517, 1491, 1437, 1397, 1326, 1177, 1123, 1099, 1067 (C=S, thioamide), 1012, 824, 769, 711. ^{1}H NMR (600 MHz, $CDCl_3$) δ 11.66 (s, 1H), 10.89 (s, 1H), 8.35 (d, J = 7.9 Hz, 1H), 8.03 (d, J = 8.8 Hz, 2H), 7.88–7.78 (m, 2H), 7.60 (ddd, J = 8.1, 5.9, 2.3 Hz, 1H), 7.45 (d, J = 8.8 Hz, 2H). ^{13}C NMR (150 MHz, $CDCl_3$) δ 179.70, 160.49, 146.44, 143.94, 136.33, 135.14, 132.53, 129.34, 128.87, 128.22, 127.18, 123.50, 122.40. HR-MS (ESI) calcd. For $C_{15}H_{11}ClN_3OS$ [$(M + H)^+$]: 316.0311; found: 316.0292. Purity > 95% (HPLC, see in ESI†).

***N*-(3-Chlorophenyl)-4-oxo-3,4-dihydroquinazoline-2-carbothioamide (8e).** Compound **8e** was synthesized by the above procedure using 3-chloroaniline **11e** as an arylamine. Pale yellow solid. Yield: 67%. M.p.: 193–201 °C. IR (KBr, cm^{-1}): ν 3441 (N–H, amide), 3249 (N–H, thioamide), 3061, 2958, 1681 (C=O, amide), 1604, 1522, 1480, 1408, 1378, 1324, 1180, 1069 (C=S, thioamide), 955, 885, 748. ^{1}H NMR (600 MHz, $CDCl_3$) δ 11.68 (s, 1H), 10.90 (s, 1H), 8.37 (d, J = 7.8 Hz, 1H), 8.18 (t, J = 2.1 Hz, 1H), 7.94 (dd, J = 7.9, 2.2 Hz, 1H), 7.90–7.82 (m, 2H), 7.62 (ddd, J = 8.2, 5.5, 2.8 Hz, 1H), 7.43 (t, J = 8.1 Hz, 1H), 7.33 (dd, J = 8.0, 1.4 Hz, 1H). ^{13}C NMR (125 MHz, $CDCl_3$) δ 180.02, 160.46, 146.41, 143.86, 138.85, 135.15, 134.94, 130.24, 128.92, 128.26, 127.46, 127.21, 122.46, 122.18, 120.33. HR-MS (ESI) calcd. For $C_{15}H_{11}ClN_3OS$ [$(M + H)^+$]: 316.0311; found: 316.0308.

***N*-(2-Chlorophenyl)-4-oxo-3,4-dihydroquinazoline-2-carbothioamide (8f).** Compound **8f** was synthesized by the above procedure using 2-chloroaniline **11f** as an arylamine. Pale yellow solid. Yield: 52%. M.p.: 216–222 °C. IR (KBr, cm^{-1}): ν 3364 (N–H, amide), 3260 (N–H, thioamide), 3179, 3071, 1709 (C=O, amide), 1602, 1526, 1468, 1438, 1407, 1324, 1127, 1070 (C=S, thioamide), 735. ^{1}H NMR (600 MHz, $CDCl_3$) δ 12.29 (s, 1H), 10.89 (s, 1H), 9.01 (dd, J = 8.3, 1.6 Hz, 1H), 8.37 (dd, J = 7.9, 1.5 Hz, 1H), 7.94–7.81 (m, 2H), 7.62 (ddd, J = 8.2, 6.7, 1.6 Hz, 1H), 7.55 (dd, J = 8.0, 1.5 Hz, 1H), 7.42 (td, J = 7.8, 1.5 Hz, 1H), 7.29 (td, J = 7.7, 1.5 Hz, 1H). ^{13}C NMR (125 MHz, $CDCl_3$) δ 179.96, 160.62, 146.52, 144.10, 135.09, 134.77, 129.88, 128.89, 128.61, 127.91, 127.45, 127.12, 126.70, 122.83, 122.46. HR-MS (ESI) calcd. For $C_{15}H_{11}ClN_3OS$ [$(M + H)^+$]: 316.0311; found: 316.0292.

***N*-(4-Bromophenyl)-4-oxo-3,4-dihydroquinazoline-2-carbothioamide (8g).** Compound **8g** was synthesized by the above procedure using 4-bromoaniline **11g** as an arylamine. Pale yellow solid. Yield: 82%. M.p.: 195–197 °C. IR (KBr, cm^{-1}): ν 3449 (N–H, amide), 3267 (N–H, thioamide), 3189, 3089, 1684, 1603 (C=O, thioamide), 1534, 1492, 1394, 1328, 1069 (C=S, thioamide), 1012, 824, 772, 714. ^{1}H NMR (600 MHz, $CDCl_3$) δ 11.65 (s, 1H), 10.88 (s, 1H), 8.38–8.28 (m, 1H), 8.02–7.93 (m, 2H), 7.88–7.79 (m, 2H), 7.65–7.56 (m, 3H). ^{13}C NMR (150 MHz, $CDCl_3$) δ 179.62, 160.42, 146.41, 143.93, 136.81, 135.12, 132.31, 128.87, 128.22, 127.19, 123.66, 122.41, 120.35. HR-MS (ESI) calcd. For $C_{15}H_{11}BrN_3OS$ [$(M + H)^+$]: 359.9806; found: 359.9797. Purity > 98% (HPLC, see in ESI†).

***N*-(4-Fluorophenyl)-4-oxo-3,4-dihydroquinazoline-2-carbothioamide (8h).** Compound **8h** was synthesized by the above procedure using 4-fluoroaniline **11h** as an arylamine. Pale yellow solid. Yield: 42%. M.p.: 198–199 °C. IR (KBr, cm^{-1}): ν 3421 (N–H, amide), 3234 (N–H, thioamide), 3067, 2918, 1688 (C=O, amide), 1602, 1523, 1478, 1435, 1410, 1382, 1327, 1239, 1177, 1124, 1067 (C=S, thioamide), 829, 747. ^{1}H NMR (600 MHz, $CDCl_3$) δ 11.63 (s, 1H), 10.93 (s, 1H), 8.40–8.33 (m, 1H), 8.07–7.98 (m, 2H), 7.88–7.79 (m, 2H), 7.61 (ddd, J = 8.2, 6.0, 2.4 Hz, 1H), 7.21–7.17 (m, 2H). ^{13}C NMR (150 MHz, $CDCl_3$) δ 179.83, 160.96 (d, J = 248.85 Hz), 160.47, 146.50, 144.00, 135.10, 133.90 (d, J = 3.4 Hz), 128.81, 128.21, 127.20, 124.39 (d, J = 8.2 Hz), 122.45, 116.21, 116.06. HR-MS (ESI) calcd. For $C_{15}H_{11}FN_3OS$ [$(M + H)^+$]: 300.0607; found: 300.0592.

***N*-(4-Nitrophenyl)-4-oxo-3,4-dihydroquinazoline-2-carbothioamide (8i).** Compound **8i** was synthesized by the above procedure using 4-nitroaniline **11i** as an arylamine. Yellow solid. Yield: 60%. M.p.: 215–222 °C. IR (KBr, cm^{-1}): ν 3359 (N–H, amide), 3190 (N–H, thioamide), 2917, 2849, 1702 (C=O, amide), 1595, 1549, 1509, 1481, 1446, 1375, 1334 (C–NO_2), 1108, 1067 (C=S, thioamide), 947, 849, 765. ^{1}H NMR (600 MHz, $CDCl_3$) δ 11.95 (s, 1H), 10.80 (s, 1H), 8.47–8.22 (m, 5H), 7.97–7.78 (m, 2H), 7.71–7.54 (m, 1H). ^{13}C NMR (125 MHz, $CDCl_3$) δ 180.79, 160.39, 146.16, 145.41, 143.71, 142.95, 135.31, 129.25, 128.33, 127.32, 125.07, 122.52, 121.87. HR-MS (ESI) calcd. For $C_{15}H_{11}N_4O_3S$ [$(M + H)^+$]: 327.0552; found: 327.0545.

4-Oxo-*N*-(4-(trifluoromethyl)phenyl)-3,4-dihydroquinazoline-2-carbothioamide (8k). Compound **8k** was synthesized by the above procedure using 4-(trifluoromethyl)aniline **11k** as an arylamine. Pale yellow solid. Yield: 81%. M.p.: 174–175 °C. IR (KBr, cm^{-1}): ν 3447 (N–H, amide), 3262 (N–H, thioamide), 3184, 2916, 1681 (C=O, amide), 1602, 1535, 1479, 1437, 1386, 1315, 1241, 1167, 1111, 1071 (C=S, thioamide), 840, 761, 716. ^{1}H NMR (600 MHz, $CDCl_3$) δ 11.78 (s, 1H), 10.84 (s, 1H), 8.34 (d, J = 7.8 Hz, 1H), 8.22 (d, J = 8.5 Hz, 2H), 7.88–7.81 (m, 2H), 7.74 (d, J = 8.4 Hz, 2H), 7.63–7.57 (m, 1H). ^{13}C NMR (150 MHz, $CDCl_3$) δ 180.53, 160.52, 146.42, 143.92, 140.73, 135.31, 129.13, 129.08 (q, J = 32.9 Hz), 128.40, 127.32, 126.59 (q, J = 4.1 Hz), 123.82 (q, J = 272.2 Hz), 122.56, 122.18. HR-MS (ESI) calcd. For

$C_{16}H_{11}F_3N_3OS$ [$(M + H)^+$]: 350.0575; found: 350.0558. Purity > 94% (HPLC, see in ESI†).

4-Oxo-*N*-(3-(trifluoromethyl)phenyl)-3,4-dihydroquinazoline-2-carbothioamide (8l). Compound **8l** was synthesized by the above procedure using 3-(trifluoromethyl)aniline **11l** as an arylamine. Yellow solid. Yield: 49%. M.p.: 153–159 °C. IR (KBr, cm^{-1}): ν 3405 (N–H, amide), 3239 (N–H, thioamide), 3151, 3033, 1672 (C=O, amide), 1598, 1529, 1431, 1332, 1167, 1067 (C=S, thioamide), 884, 774, 696. ^{1}H NMR (600 MHz, DMSO-d_6) δ 12.70 (s, 1H), 12.06 (s, 1H), 8.41 (s, 1H), 8.22 (t, J = 8.2 Hz, 2H), 7.94 (t, J = 7.0 Hz, 1H), 7.88 (d, J = 7.9 Hz, 1H), 7.75 (t, J = 7.8 Hz, 1H), 7.72 (d, J = 8.0 Hz, 1H), 7.66 (t, J = 7.4 Hz, 1H). ^{13}C NMR (150 MHz, DMSO-d_6) δ 186.14, 161.16, 149.38, 147.44, 139.72, 135.55, 130.63, 129.86 (q, J = 31.8 Hz), 128.74, 128.46, 128.03, 126.67, 124.33 (q, J = 272.3 Hz), 123.95 (d, J = 3.6 Hz), 122.41, 120.59 (q, J = 3.5 Hz). HR-MS (ESI) calcd. For $C_{16}H_{11}F_3N_3OS$ [$(M + H)^+$]: 350.0575; found: 350.0560.

***N*-(3-Cyanophenyl)-4-oxo-3,4-dihydroquinazoline-2-carbothioamide (8m).** Compound **8m** was synthesized by the above procedure using 3-cyanoaniline **11m** as an arylamine. Pale yellow solid. Yield: 44%. M.p.: 229–230 °C. IR (KBr, cm^{-1}): ν 3429 (N–H, amide), 3268 (N–H, thioamide), 3073, 2960, 2233, 1684 (C=O, amide), 1604, 1534, 1481, 1432, 1380, 1318, 1070 (C=S, thioamide), 878, 796, 767. ^{1}H NMR (600 MHz, $CDCl_3$) δ 11.75 (s, 1H), 10.82 (s, 1H), 8.51–8.49 (m, 1H), 8.40–8.33 (m, 1H), 8.28 (dt, J = 6.8, 2.4 Hz, 1H), 7.90–7.83 (m, 2H), 7.66–7.59 (m, 3H)·^{13}C NMR (125 MHz, $CDCl_3$) δ 180.84, 160.37, 146.26, 143.70, 138.55, 135.23, 130.56, 130.20, 129.10, 128.28, 127.27, 126.41, 125.35, 122.52, 117.81, 113.55. HR-MS (ESI) calcd. For $C_{16}H_{11}N_4OS$ [$(M + H)^+$]: 307.0654; found: 307.0640.

Methyl 4-(4-oxo-3,4-dihydroquinazoline-2-carbothioamido) benzoate (8n). Compound **8n** was synthesized by the above procedure using 4-(carbomethoxy)aniline **11n** as an arylamine. Pale yellow solid. Yield: 42%. M.p.: 200–201 °C. IR (KBr, cm^{-1}): ν 3417 (N–H, amide), 3278 (N–H, thioamide), 3184, 3098, 2955, 1693 (C=O, amide), 1599, 1534, 1436, 1391, 1281, 1110 (C=S, thioamide), 849, 772, 708. ^{1}H NMR (600 MHz, $CDCl_3$) δ 11.83 (s, 1H), 10.88 (s, 1H), 8.36 (d, J = 7.9 Hz, 1H), 8.21 (d, J = 8.8 Hz, 2H), 8.16 (d, J = 8.8 Hz, 2H), 7.85 (d, J = 3.3 Hz, 2H), 7.65–7.58 (m, 1H), 3.95 (s, 3H). ^{13}C NMR (125 MHz, $CDCl_3$) δ 179.96, 166.06, 160.44, 146.36, 143.90, 141.51, 135.16, 130.82, 128.96, 128.57, 128.28, 127.21, 122.44, 121.41, 52.29. HR-MS (ESI) calcd. For $C_{17}H_{14}N_3O_3S$ [$(M + H)^+$]: 340.0756; found: 340.0745.

General procedure for the synthesis of 3,4-dihydroquinazoline-2-carbothioamide derivatives (8o, 8p)

A mixture of **10** (1.0 mmol), benzylamine **11o**, **11p** (1.0 mmol), sulfur (40 mg, 1.25 mmol), and acetic acid (60 mg, 1 mmol) in DMSO (0.5 mL) was heated in a 7 mL test tube sealed with a rubber stopper, at 100 °C for 16 h. The crude mixture was purified by column chromatography on silica gel (acetone : *n*-hexane = 3% to 5%, v/v) to obtain **8o**, **8p** compounds.[44]

***N*-Benzyl-4-oxo-3,4-dihydroquinazoline-2-carbothioamide (8o).** Compound **8o** was synthesized by the above procedure using benzylamine **11o** as a benzylamine. Pale yellow solid. Yield: 28%. M.p.: 164–165 °C. IR (KBr, cm^{-1}): ν 3460 (N–H, amide), 3256 (N–H, thioamide), 3026, 2947, 1681 (C=O, amide), 1606, 1535, 1482, 1431, 1331, 1241, 1179, 1131, 1100, 1070 (C=S, thioamide), 1014, 826, 756. ^{1}H NMR (600 MHz, $CDCl_3$) δ 10.86 (s, 1H), 10.08 (s, 1H), 8.33 (dd, J = 7.9, 1.5 Hz, 1H), 7.81–7.75 (m, 1H), 7.73 (d, J = 8.2 Hz, 1H), 7.59–7.54 (m, 1H), 7.46–7.34 (m, 5H), 5.00 (d, J = 5.8 Hz, 2H). ^{13}C NMR (150 MHz, $CDCl_3$) δ 183.73, 160.48, 146.83, 143.52, 135.33, 134.92, 129.11, 128.60, 128.43, 128.34, 128.26, 127.07, 122.61, 50.38. HR-MS (ESI) calcd. For $C_{16}H_{14}N_3OS$ [$(M + H)^+$]: 296.0858; found: 296.0843.

***N*-(4-Chlorobenzyl)-4-oxo-3,4-dihydroquinazoline-2-carbothioamide (8p).** Compound **8p** was synthesized by the above procedure using 4-chlorobenzylamine **11p** as a benzylamine. Yellow solid. Yield: 36%. M.p.: 184–186 °C. IR (KBr, cm^{-1}): ν 3442 (N–H, amide), 3262 (N–H, thioamide), 3185, 2916, 2848, 1680 (C=O, amide), 1602, 1535, 1479, 1436, 1385, 1314, 1167, 1111, 1071 (C=S, thioamide), 840, 760. ^{1}H NMR (600 MHz, $CDCl_3$) δ 10.83 (s, 1H), 10.08 (s, 1H), 8.34 (dd, J = 7.9, 1.5 Hz, 1H), 7.82–7.76 (m, 1H), 7.73 (d, J = 8.2 Hz, 1H), 7.61–7.55 (m, 1H), 7.41–7.32 (m, 4H), 4.98 (d, J = 5.9 Hz, 2H). ^{13}C NMR (150 MHz, $CDCl_3$) δ 184.02, 160.45, 146.75, 143.45, 134.97, 134.37, 133.80, 129.65, 129.25, 128.69, 128.25, 127.09, 122.62, 49.45. HR-MS (ESI) calcd. For $C_{16}H_{13}ClN_3OS$ [$(M + H)^+$]: 330.0468; found: 330.0453.

Synthesis of 3,4-dihydroquinazoline-2-carboxamide derivative (8q)

Compound **8q** was synthesized based on a procedure previously described by Thanh Binh Nguyen *et al.*[48] Brief, a mixture of **10** (1 mmol), 4-(trifluoromethyl)aniline **11k** (1 mmol), $FeCl_2 \cdot 4H_2O$ (5 mol%), and sulfur (1.25 mmol, 40 mg) in DMSO (0.3 mL) was carried out in a 7 mL test tube sealed with a rubber stopper, at 120 °C for 16 h. The crude mixture was purified by column chromatography on silica gel (eluted with a mixture of EtOAc : *n*-hexane = 10%, v/v) to obtain compound **8q**.

4-Oxo-*N*-(4-(trifluoromethyl)phenyl)-3,4-dihydroquinazoline-2-carboxamide (8q). White solid. Yield: 43%. M.p.: 253–254 °C. IR (KBr, cm^{-1}): ν 3332 (N–H, amide), 3188, 1669 (C=O, amide), 1604, 1535, 1479, 1412, 1332, 1164, 1105, 1072, 1017, 894, 843, 774. ^{1}H NMR (600 MHz, DMSO-d_6) δ 12.55 (s, 1H), 11.11 (s, 1H), 8.22 (d, J = 7.8 Hz, 1H), 8.13 (d, J = 8.4 Hz, 2H), 7.97–7.89 (m, 2H), 7.78 (d, J = 8.5 Hz, 2H), 7.70–7.63 (m, 1H). ^{13}C NMR (150 MHz, DMSO-d_6) δ 161.43, 159.14, 147.33, 146.16, 141.79, 135.31, 128.89, 128.42, 126.71, 126.50 (q, J = 3.5 Hz), 125.64 (d, J = 271.2 Hz), 125.03 (q, J = 32.7 Hz), 123.35, 121.14. HR-MS (ESI) calcd. For $C_{16}H_{11}F_3N_3O_2$ [$(M + H)^+$]: 334.0803; found: 334.0796.

In vitro anti-inflammatory activity

The *in vitro* anti-inflammatory activity of the tested compounds was evaluated by inhibiting NO production in LPS-stimulated RAW 264.7 cells following a similar procedure described by Diep Trinh Thi.[63] Briefly, RAW 274.7 cells were seeded into 96-well plates at a concentration of 2 × 105 cells per well and cultured in an incubator at 37 °C and 5% CO_2 for 24 h. The sample was dissolved in 100% DMSO to an initial concentration of 20 mM. The sample was diluted in a 96-well plate with cell culture medium (without FBS) into 4 concentration ranges from

high to low. Cells were then incubated with different concentrations for 2 h before being stimulated to produce NO with LPS (10 μg mL^{-1}) for 24 h. Some wells were not incubated with samples but only used sample diluent as negative controls. While the positive controls used were dexamethasone (Sigma) at concentrations of 100; 20; 4 and 0.8 μM. Nitrite (NO_2^-), considered an indicator for NO production, was determined using the Griess Reagent System (Promega Cooperation, WI, USA). Specifically, 100 μL of cell culture medium (incubation sample) was transferred to a new 96-well plate and 100 μL of Griess reagent was added: 50 μL of 1% (w/v) sulfanilamide in 5% (v/v) phosphoric acid and 50 μL of 0.1% (w/v) *N*-1-naphthylethylenediamine dihydrochloride in water. The mixture was further incubated at room temperature for 10 min and the nitrite content was measured using a microplate reader at 540 nm. DMEM medium without FBS was used as the blank well. The nitrite content of each experimental sample was determined by the $NaNO_2$ standard curve and compared in % with the negative control sample (LPS). The corresponding NO production inhibition ability of the sample was determined by the formula: (%) inhibition = 100% − [content NO_{sample}/content NO_{LPS}] × 100. The test was repeated 3 times to ensure accuracy. The IC_{50} value (concentration that inhibits 50% of NO formation) was determined using the computer software TableCurve 2Dv4.

Molecular docking studies

Since the experiments in this research were performed on RAW264.7 cells, the crystal structure of mouse TLR4 and mouse MD-2 complex were selected for docking simulation with studied compounds. The X-ray crystallographic model of the complexes was downloaded from the RCSB Protein Data Bank (PDB ID: 2Z64).[64] A resolution between 1.5 and 3.0 Å is considered a good quality for docking studies.[65,66] The interaction with model 2Z64, a monomeric LPS-free TLR4-MD-2 structure that acted as an inactive conformation prepared for ligand docking, was the primary basis for identifying the putative binding region. Then, the active conformation (PDB ID: 3VQ2), a dimeric TLR4/MD-2 combination with LPS, was subsequently used to confirm the results. To create a free receptor, water molecules were removed from the protein. The protein was prepared for docking simulations by assigning partial charges, solvation parameters, and hydrogens to the receptor molecule. A grid box was constructed to encompass all possible binding sites by using validated ligands as references. AutoDock 4.2 was utilized for the molecular docking simulation using Lamarckian Genetic Algorithm (LGA). The ligand conformation with the lowest binding free energy, selected from the most favored cluster, was chosen for further analysis. The results from the AutoDock modeling studies were analyzed using PyMOL[67] and Discovery Studio Visualizer.[68]

Conclusions

A library of 15 novel quinazoline-4(3*H*)-one derivatives functionalized at position 2nd *via* thioamide linkages attached to phenyl and benzyl rings was successfully designed and synthesized in two simple steps. Interestingly, compounds with potent *in vitro* anti-inflammatory activity were synthesized in good yields (62–82%). Such as compounds **8a**, **8d**, **8g** and **8k**. The structures of the synthesized compounds were determined by modern physicochemical analysis methods such as IR, NMR, HRMS, and melting point. These compounds were also evaluated for their anti-inflammatory activity through their ability to inhibit NO production. Compounds **8d**, **8g**, and **8k** exhibited superior anti-inflammatory activity compared to the standard drug dexamethasone. Compound **8a** inhibited the inflammatory mediator NO equivalently to dexamethasone. SAR studies demonstrated the importance of the presence of a thioamide linker with a phenyl ring attached to halogen-containing substituents at the *para*-position in the generation of novel quinazolinone compounds with potent anti-inflammatory activity. *In silico* studies showed that candidates **8d**, **8g**, and **8k** were potent inhibitors of TLR4 signaling with significant docking scores of −7.71, −7.65, and −7.84 kcal mol^{-1}, respectively, compared to −7.10 kcal mol^{-1} of dexamethasone. One of the outstanding features of our NO inhibitor essential for high potency is the presence of a thioamide group, as its replacement by an amide results in a sharp decrease in inhibitory activity. This highlights the important role of favorable sulfur interactions in protein-ligand complexes, as well as the thioamide group in drug design. Finally, physicochemical and ADMET studies of the potent compounds were also conducted, showing that they had favorable ADMET profiles, *in silico* studies of the lead compounds demonstrate their potential as drug candidates.

Data availability

The data supporting this article are available within the article and its ESI.†

Conflicts of interest

There are no conflicts to declare.

Acknowledgements

This research is funded by Vietnam National Foundation for Science and Technology Development (NAFOSTED) under grant number 104.01-2020.49.

References

1 V. Ngoc Binh, S. Adorisio, D. V. Delfino and Q. A. Ngo, *Prod. Commun.*, 2022, **17**, 1934578X221105692.
2 C.-L. Hsu, S.-C. Fang and G.-C. Yen, *Food Funct.*, 2013, **4**, 1216–1222.
3 M. E. Bauer and A. L. Teixeira, *Ann. N. Y. Acad. Sci.*, 2019, **1437**, 57–67.
4 S. U. Rahman, Y. Li, Y. Huang, L. Zhu, S. Feng, J. Wu and X. Wang, *Inflammopharmacology*, 2018, **26**, 319–330.
5 P. Tripathi, P. Tripathi, L. Kashyap and V. Singh, *FEMS Microbiol. Immunol.*, 2007, **51**, 443–452.

6 M. Marra, A. Mariconda, D. Iacopetta, J. Ceramella, A. D'Amato, C. Rosano, K. Tkachenko, M. Pellegrino, S. Aquaro, M. S. Sinicropi and P. Longo, *Molecules*, 2024, **29**, 5262.
7 L.-R. Balahura Stămat and S. Dinescu, *Sci. Rep.*, 2024, **14**, 24753.
8 J. N. Sharma, A. Al-Omran and S. S. Parvathy, *Inflammopharmacology*, 2007, **15**, 252–259.
9 S. Sharma, D. Kumar, G. Singh, V. Monga and B. Kumar, *Eur. J. Med. Chem.*, 2020, **200**, 112438.
10 M. Bian, Q.-q. Ma, Y. Wu, H.-h. Du and G. Guo-hua, *J. Enzyme Inhib. Med. Chem.*, 2021, **36**, 2139–2159.
11 M. Bhat, S. L. Belagali, S. V. Mamatha, B. K. Sagar and E. V. Sekhar, in *Studies in Natural Products Chemistry*, ed. R. Atta ur, Elsevier, 2021, vol. 71, pp. 185–219.
12 A. R. Awwad and K. A. Fars, in *Quinazolinone and Quinazoline Derivatives*, ed. A.-k. Ali Gamal, IntechOpen, Rijeka, 2020, ch. 2, pp. 11–38.
13 M. F. Zayed, *ChemEngineering*, 2022, **6**, 94.
14 T. C. Moon, M. Murakami, I. Kudo, K. H. Son, H. P. Kim, S. S. Kang and H. W. Chang, *Inflammation Res.*, 1999, **48**, 621–625.
15 S. Jia and C. Hu, *Molecules*, 2010, **15**, 1873–1881.
16 K. M. Amin, M. M. Kamel, M. M. Anwar, M. Khedr and Y. M. Syam, *Eur. J. Med. Chem.*, 2010, **45**, 2117–2131.
17 A. Kumar and C. S. Rajput, *Eur. J. Med. Chem.*, 2009, **44**, 83–90.
18 B. A. Rather, T. Raj, A. Reddy, M. P. S. Ishar, S. Sivakumar and P. Paneerselvam, *Arch. Pharm.*, 2010, **343**, 108–113.
19 A. Sakr, S. Rezq, S. M. Ibrahim, E. Soliman, M. M. Baraka, D. G. Romero and H. Kothayer, *J. Enzyme Inhib. Med. Chem.*, 2021, **36**, 1810–1828.
20 S. K. Verma, R. Verma, K. P. Rakesh and D. C. Gowda, *Eur. J. Med. Chem. Rep.*, 2022, **6**, 100087.
21 S. Kerdphon, N. Khamto, K. Buddhachat, J. Ngoenkam, P. Paensuwan, S. Pongcharoen, T. Singh, P. Meepowpan and J. Jongcharoenkamol, *ACS Med. Chem. Lett.*, 2023, **14**, 1167–1173.
22 A. M. Alsibaee, H. M. Al-Yousef and H. S. Al-Salem, *Molecules*, 2023, **28**, 978.
23 S. Asirvatham, B. V. Dhokchawle and S. J. Tauro, *Arabian J. Chem.*, 2019, **12**, 3948–3962.
24 C. K. Khatri, K. S. Indalkar, C. R. Patil, S. N. Goyal and G. U. Chaturbhuj, *Bioorg. Med. Chem. Lett.*, 2017, **27**, 1721–1726.
25 M. H. Abdelrahman, B. G. M. Youssif, M. A. abdelgawad, A. H. Abdelazeem, H. M. Ibrahim, A. E. G. A. Moustafa, L. Treamblu and S. N. A. Bukhari, *Eur. J. Med. Chem.*, 2017, **127**, 972–985.
26 A. Sakr, H. Kothayer, S. M. Ibrahim, M. M. Baraka and S. Rezq, *Bioorg. Chem.*, 2019, **84**, 76–86.
27 K. Vinaya, R. Naika, C. S. A. Kumar, S. R. Ranganath, S. B. B. Prasad, V. Krishna and K. S. Rangappa, *Arch. Pharm.*, 2009, **342**, 476–483.
28 S. Kumari, A. V. Carmona, A. K. Tiwari and P. C. Trippier, *J. Med. Chem.*, 2020, **63**, 12290–12358.
29 N. Mahanta, D. M. Szantai-Kis, E. J. Petersson and D. A. Mitchell, *ACS Chem. Biol.*, 2019, **14**, 142–163.
30 A. Choudhary and R. T. Raines, *ChemBioChem*, 2011, **12**, 1801–1807.
31 P. Ghosh, N. Raj, H. Verma, M. Patel, S. Chakraborti, B. Khatri, C. M. Doreswamy, S. R. Anandakumar, S. Seekallu, M. B. Dinesh, G. Jadhav, P. N. Yadav and J. Chatterjee, *Nat. Commun.*, 2023, **14**, 6050.
32 K. Tsuji, T. Ishii, T. Kobayakawa, N. Higashi-Kuwata, K. Shinohara, C. Azuma, Y. Miura, H. Nakano, N. Wada, S.-i. Hattori, H. Bulut, H. Mitsuya and H. Tamamura, *J. Med. Chem.*, 2023, **66**, 13516–13529.
33 S. Sharma, D. Singh, S. Kumar, Vaishali, R. Jamra, N. Banyal, Deepika, C. C. Malakar and V. Singh, *Beilstein J. Org. Chem.*, 2023, **19**, 231–244.
34 K. Pedrood, H. Azizian, M. N. Montazer, A. Moazzam, M. Asadi, H. Montazeri, M. Biglar, M. Zamani, B. Larijani, K. Zomorodian, M. Mohammadi-Khanaposhtani, C. Irajie, M. Amanlou, A. Iraji and M. Mahdavi, *Sci. Rep.*, 2022, **12**, 13827.
35 G. Huang, T. Cierpicki and J. Grembecka, *Eur. J. Med. Chem.*, 2024, **277**, 116732.
36 T. S. Jagodziński, *Chem. Rev.*, 2003, **103**, 197–228.
37 E. Korbut, M. Suski, Z. Śliwowski, D. Bakalarz, U. Głowacka, D. Wójcik-Grzybek, G. Ginter, K. Krukowska, T. Brzozowski, M. Magierowski, J. L. Wallace and K. Magierowska, *Inflammopharmacology*, 2024, **32**, 2049–2060.
38 E. Gugliandolo, R. Fusco, R. D'Amico, A. Militi, G. Oteri, J. L. Wallace, R. Di Paola and S. Cuzzocrea, *Pharmacol. Res.*, 2018, **132**, 220–231.
39 U. Głowacka, K. Magierowska, D. Wójcik, J. Hankus, M. Szetela, J. Cieszkowski, E. Korbut, A. Danielak, M. Surmiak, A. Chmura, J. L. Wallace and M. Magierowski, *Antioxid. Redox Signaling*, 2021, **36**, 189–210.
40 J. L. Wallace, D. Vaughan, M. Dicay, W. K. MacNaughton and G. de Nucci, *Antioxid. Redox Signaling*, 2017, **28**, 1533–1540.
41 J. R. W. Glanville, P. Jalali, J. D. Flint, A. A. Patel, A. A. Maini, J. L. Wallace, A. A. Hosin and D. W. Gilroy, *FASEB J.*, 2021, **35**, e21913.
42 T. Murai, in *Chemistry of Thioamides*, ed. T. Murai, Springer Singapore, Singapore, 2019, pp. 45–73.
43 Q. Zhang, L. Soulère and Y. Queneau, *Molecules*, 2023, **28**, 3527.
44 T. T. T. Nguyen, L. A. Nguyen, Q. A. Ngo, M. Koleski and T. B. Nguyen, *Org. Chem. Front.*, 2021, **8**, 1593–1598.
45 J. Sun, T. Tao, D. Xu, H. Cao, Q. Kong, X. Wang, Y. Liu, J. Zhao, Y. Wang and Y. Pan, *Tetrahedron Lett.*, 2018, **59**, 2099–2102.
46 S. Yoshida, T. Aoyagi, S. Harada, N. Matsuda, T. Ikeda, H. Naganawa, M. Hamada and T. Takeuchi, *J. Antibiot.*, 1991, **44**, 111–112.
47 X. Yu, L. Gao, L. Jia, Y. Yamamoto and M. Bao, *J. Org. Chem.*, 2018, **83**, 10352–10358.
48 T. T. T. Nguyen, V. D. Duong, T. N. N. Pham, Q. T. Duong and T. B. Nguyen, *Org. Biomol. Chem.*, 2022, **20**, 8054–8058.

49 N. Pirnazarova, U. Yakubov, S. Allabergenova, A. Tojiboev, K. Turgunov and B. Elmuradov, *Acta Crystallogr., Sect. E:Crystallogr. Commun.*, 2022, **78**, 47–50.
50 B. Khatri, S. Raghunathan, S. Chakraborti, R. Rahisuddin, S. Kumaran, R. Tadala, P. Wagh, U. D. Priyakumar and J. Chatterjee, *Angew. Chem., Int. Ed.*, 2021, **60**, 24870–24874.
51 M. Nibin Joy, M. R. Guda and G. V. Zyryanov, *Pharmaceuticals*, 2023, **16**, 1326.
52 T. Khan, S. Dixit, R. Ahmad, S. Raza, I. Azad, S. Joshi and A. R. Khan, *J. Chem. Biol.*, 2017, **10**, 91–104.
53 F. Cheng, W. Li, Y. Zhou, J. Shen, Z. Wu, G. Liu, P. W. Lee and Y. Tang, *J. Chem. Inf. Model.*, 2012, **52**, 3099–3105.
54 A. T. Garcia-Sosa, U. Maran and C. Hetenyi, *Curr. Med. Chem.*, 2012, **19**, 1646–1662.
55 N. T. Dan, H. D. Quang, V. Van Truong, D. Huu Nghi, N. M. Cuong, T. D. Cuong, T. Q. Toan, L. G. Bach, N. H. T. Anh, N. T. Mai, N. T. Lan, L. Van Chinh and P. M. Quan, *Sci. Rep.*, 2020, **10**, 11429.
56 S. T. Ngo, N. M. Tam, M. Q. Pham and T. H. Nguyen, *J. Chem. Inf. Model.*, 2021, **61**, 2302–2312.
57 N. T. Nguyen, T. H. Nguyen, T. N. H. Pham, N. T. Huy, M. V. Bay, M. Q. Pham, P. C. Nam, V. V. Vu and S. T. Ngo, *J. Chem. Inf. Model.*, 2019, **60**, 204–211.
58 Q. A. Ngo, T. H. N. Thi, M. Q. Pham, D. Delfino and T. T. Do, *Mol. Diversity*, 2021, **25**, 2307–2319.
59 X. Lin, J. Zhang, D. Fan, J. Hou, H. Wang, L. Zhu, R. Tian, X. An and M. Yan, *Front. Pharmacol.*, 2021, **12**, 643188.
60 M.-q. Tao, C.-l. Ji, Y.-j. Wu, J.-y. Dong, Y. Li, O. J. Olatunji and J. Zuo, *Inflammation*, 2020, **43**, 1821–1831.
61 X. Gong, Y. He, D. Yang, S. Yang, J. Li, H. Zhao, Q. Chen, Q. Ren and B. Zhang, *Bioorg. Chem.*, 2022, **127**, 105939.
62 T. Chen, Y. Zhou, D. Han, L.-B. Han and S.-F. Yin, *Org. Biomol. Chem.*, 2014, **12**, 3802–3807.
63 D. Trinh Thi, D. Luong Van, T. Phung Van, H. Nguyen Thi, T. Do Thi, U. Nguyen Thi To, L. Tran Thi Hoai, K. Dang Vinh, T. T. Huynh and T. Le Thi Thanh, *Nat. Prod. Res.*, 2024, **38**, 1834–1843.
64 H. M. Kim, B. S. Park, J.-I. Kim, S. E. Kim, J. Lee, S. C. Oh, P. Enkhbayar, N. Matsushima, H. Lee, O. J. Yoo and J.-O. Lee, *Cell*, 2007, **130**, 906–917.
65 C. Didierjean and F. Tête-Favier, *Acta Crystallogr., Sect. D:Struct. Biol.*, 2016, **72**, 1308–1309.
66 C. Venugopal, C. Demos, K. Jagannatha Rao, M. Pappolla and K. Sambamurti, *CNS Neurol. Disord.: Drug Targets*, 2008, **7**, 278–294.
67 L. Schrödinger, *The PyMOL Molecular Graphics System, Version 1.3r1*, 2010.
68 BIOVIA, *Dassault Systèmes. Discovery Studio Visualizer, v21.1.0.20298*, 2021.